

Conformal models of de Sitter space, initial conditions for inflation and the CMB

Anthony Lasenby¹ and Chris Doran²

Astrophysics Group, Cavendish Laboratory, Madingley Road,
Cambridge CB3 0HE, UK.

Abstract

Conformal embedding of closed-universe models in a de Sitter background suggests a quantisation condition on the available conformal time. This condition implies that the universe is closed at no greater than the 10% level. When a massive scalar field is introduced to drive an inflationary phase this figure is reduced to closure at nearer the 1% level. In order to enforce the constraint on the available conformal time we need to consider conditions in the universe before the onset of inflation. A formal series around the initial singularity is constructed, which rests on a pair of dimensionless, scale-invariant parameters. For physically-acceptable models we find that both parameters are of order unity, so no fine tuning is required, except in the mass of the scalar field. For typical values of the input parameters we predict the observed values of the cosmological parameters, including the magnitude of the cosmological constant. The model produces a very good fit to the most recent CMBR data, predicting a low- ℓ fall-off in the CMB power spectrum consistent with that observed by WMAP.

1 Introduction

Experimental evidence is now strongly in favour of the idea that a non-zero cosmological constant, or some form of ‘dark energy’, is currently responsible for around 70% of the total energy density of the universe [1]. There have been many theoretical attempts to justify the reintroduction of a Λ -term, something that was once viewed as a rather ugly and unnecessary extension to classical general relativity. Many of these are based on ideas from particle physics, including concepts such as spontaneous symmetry breaking and false vacua. These ideas can successfully explain the size of the cosmological ‘constant’ required during an inflationary phase, but all such models have great difficulty in explaining the current scale of the cosmological constant without implausible levels of fine tuning.

It could be argued that the current scale of the cosmological constant suggests that its role may be more geometric, rather than field-theoretic. This idea fits in well with the gauge-theoretic viewpoint of gravity that we have developed elsewhere [2, 3]. In the absence of any matter, a non-zero cosmological constant implies that the universe should be described by a de Sitter space. This space should then form the background for the gauge theory treatment of gravity, though the details of such a theory remain to be fully worked out.

Here we explore some simpler consequences of the view that Λ should be viewed as a genuine *constant* with a geometric role to play. The ideas outlined

¹e-mail: a.n.lasenby@mrao.cam.ac.uk

²e-mail: c.Doran@mrao.cam.ac.uk

here are discussed in more detail in [4]. We first introduce a new picture of de Sitter geometry, which generalises the Poincaré disk picture of hyperbolic geometry [3, 5]. Since all cosmological models are conformally equivalent (they all have vanishing Weyl curvature), all cosmologies with a de Sitter end state will have a standard embedding in the conformal picture. These embeddings are revealing, and suggest a ‘preferred’ cosmology — one with closed spatial sections, in which the total available conformal time is $\pi/2$. Such a model places the initial singularity symmetrically in the centre of the de Sitter picture. The requirement on the total conformal time suggests the operation of a quantisation condition, and we speculate as to how such a condition may arise. Of course, there are many theoretical reasons for preferring spatial flatness which is, after all, supposed to be one of the main predictions of inflation. For example, there are difficulties in constructing a homogeneous stress-energy tensor for Dirac fermions in anything other than a spatially-flat universe [6, 2]. But closed universe models have their own attractive features, particularly in their inherent finiteness. Furthermore, in closed (or open) cosmologies the scale factor can be determined absolutely from the equation

$$\frac{1}{R^2} = \frac{8\pi G}{3}\rho - H^2 + \frac{\Lambda}{3}. \quad (1)$$

This result simplifies calculations for perturbations, as we do not have to track the scale factor through reheating in order to compare physical scales today with those during inflation.

Several other authors have of course been interested recently in closed universe models, motivated partly by the apparent low- ℓ turn down in the WMAP results [1]. For example, Efstathiou [7] proposed a phenomenological model in which the low- k primordial spectrum in a closed model has an exponential cut-off on a scale comparable to the curvature scale. On the other hand, Starobinsky [8], predicted that the effect of closure for adiabatic scalar perturbations was in general to increase low- ℓ values. This is clearly an area where more detailed calculations are necessary.

On the observational side, Efstathiou (e.g. [9]) and others have queried whether foreground effects on power spectrum estimation could be affecting the low- ℓ modes. However, it is likely that the low value seen for the quadrupole mode is still statistically significant, and thus represents something which needs explaining in the standard model. Other explanations which have been given include [10] which has a period of fast-roll in a flat model, and also topological attempts at explanation, via effects in a compact closed universe [11].

What we will look at here is simple closed universe, with no topological effects. But, by pursuing our boundary condition, we will find strong constraints among cosmological parameters. In particular, for a cosmological model with a given equation of state, the condition that the total elapsed conformal time is equal to $\pi/2$ singles out a unique trajectory in the $(\Omega_M, \Omega_\Lambda)$ plane. For example, a simple dust model predicts a universe that is closed at around the 10% level. This represents an upper limit, and both inflationary and radiation-dominated epochs drive this figure down. A prediction of the cosmological model can equally be interpreted as a prediction of Λ and, for typical input parameters, we find that

$$\Lambda \approx \exp(-6N)l_p^{-2}. \quad (2)$$

Here N is the number of e-foldings in the inflationary region, and turns out to be roughly 46, putting Λ in precisely the observed range.

The model of inflation we consider is the simplest available — that of a massive scalar field. This produces an extremely tight model that agrees well with all current experimental data. In order to apply our boundary condition we need to study the evolution of the scalar field from the initial singularity, through the inflationary region, before matching onto a standard cosmological model. It has become quite common in the inflationary community to ignore the initial singularity and concentrate instead on suitable initial conditions for inflation. It might have been hoped that the peculiar nature of the inflationary stress-energy tensor, which violates the weak energy condition, might circumvent some of the standard singularity theorems. But this is not the case. Inflationary models are geodesically incomplete in the past, and the cosmological equations can be easily run backwards in time to reveal the initial singularity [12, 13]. In this respect, inflation has little to say about the ‘specialness’ of the initial singularity (zero Weyl curvature) which can be regarded as one of the outstanding problems in physics [14].

Expanding the field equations around the initial singularity can be performed using an iterative scheme in powers of t and $\ln t$. The resulting series are governed by two parameters, which effectively control the degree of inflation and the curvature. Fixing both of these parameters to be of order unity produces inflationary models in a closed universe which are consistent with observation. This appears to provide a counterexample to statements that it is difficult to obtain closed universe inflation without excessive fine tuning [15, 16, 17, 18].

As the universe exits the inflationary region it evolves as if it had started from an effective big-bang, with a displaced time coordinate. Photons have travelled an appreciable distance by the end of inflation, which alters how we apply the $\pi/2$ boundary condition. The result of these effects is the imposition of a see-saw mechanism linking the current state of the universe and the initial conditions. The more we increase the number of e-folds during inflation, the smaller the value of the cosmological constant, and vice-versa. With initial conditions chosen to give the required number of e-foldings to generate the observed perturbation spectrum, we find that the predicted universe is closed at the level of a few percent, in excellent agreement with observation. More detailed calculation also reveals a dip in the low- ℓ part of the power spectrum. However, these calculations are difficult and we comment on the problems that must be overcome in order to make this prediction robust.

Unless stated otherwise we work in units where $G = c = \hbar = 1$. Where it adds clarity, factors of G are included, so that G has dimensions of (distance)².

2 Conformal pictures of de Sitter space

De Sitter space is a space of constant negative curvature, forming the Lorentzian analogue of the non-Euclidean geometry discovered by Lobachevskii and Bolyai [5, 3]. Two-dimensional non-Euclidean geometry has an elegant construction in terms of the Poincaré disc (which was, in fact, first given by Beltrami in 1868, and later rediscovered by Poincaré [14].) In the Poincaré disk model, geodesics are represented as ‘ d -lines’ — circles that intersect the disc boundary at right-angles (see figure 1). Here we develop a similar picture for 2-dimensional de

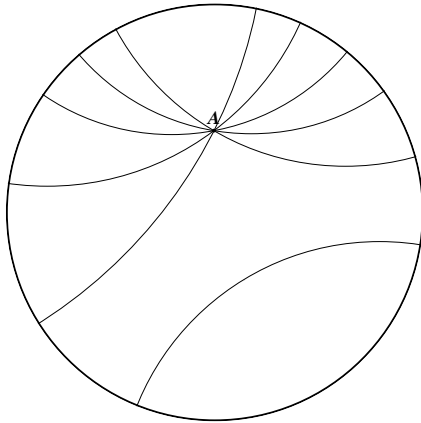


Figure 1: *The Poincaré disc.* Points inside the disc represent points in a 2-dimensional non-Euclidean (hyperbolic) space. A set of d -lines are also shown. These are (Euclidean) circles that intersect the unit circle at right angles. Given a d -line and point A not on the line, one can find an infinite number of lines through A that do not intersect the line.

Sitter space, which is sufficient to capture the key features of the geometry. We start with an embedding picture, representing de Sitter space as the 2-surface defined by

$$T^2 - X^2 - Y^2 = -a^2, \quad (3)$$

where (T, X, Y) denote coordinates in a space of signature $(1, 2)$ and a is a constant. The resulting surface is illustrated in figure 2. The figure illustrates a key property of the entire de Sitter geometry, which is that spatial sections are closed, whereas the timelike direction is open. So de Sitter space describes a closed universe that lasts for infinite time. One can set up local coordinate patches for which spatial sections are flat or open, but these coordinates are not global. These are discussed in the following section. Null geodesics are straight lines formed by the intersection of the surface and a vertical plane a distance a from the timelike axis. Despite the fact that the space is spatially closed, the furthest a photon can travel is half of the way round the universe.

The preceding picture is the ‘standard’ one of de Sitter space, though it is not the one originally put forward by de Sitter [19, 20]. Further spaces of constant curvature can be created by topological identifications, and among these is the antipodal map on spatial sections. In terms of embedding coordinates (T, X^i) , this is the map $(T, X^i) \mapsto (T, -X^i)$. The result has spatial sections of the form $\mathbb{R}P^n$ as opposed to S^n , where $\mathbb{R}P^n$ denotes the real n -dimensional projective plane. The projective plane can be quite hard to visualise. For example, $\mathbb{R}P^2$ involves taking a Möbius strip, and applying a further twisted identification on the ‘long’ side (figure 3). The resulting manifold is non-orientable, and cannot be embedded in three dimensions without self-intersection (it is similar to a Klein bottle). Of more physical relevance is $\mathbb{R}P^3$, which is orientable, though the space contains non-contractable loops and is equally hard to visualise. $\mathbb{R}P^3$ is also a group manifold, so as a background space it does have some attractive

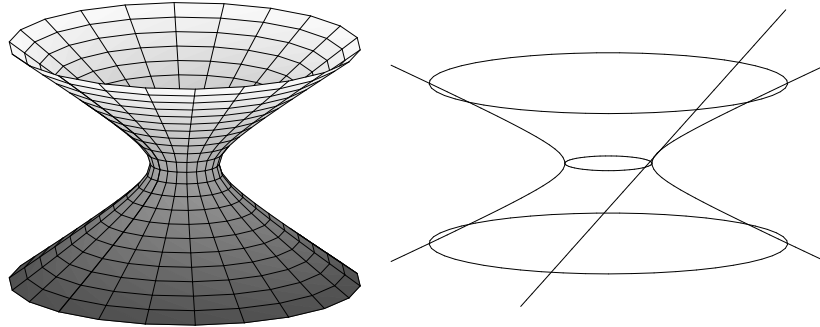


Figure 2: *Two-dimensional de Sitter Space*. The timelike direction is vertical, and spatial sections are closed. The right-hand diagram shows a null geodesic, which is a straight line in the embedding space.

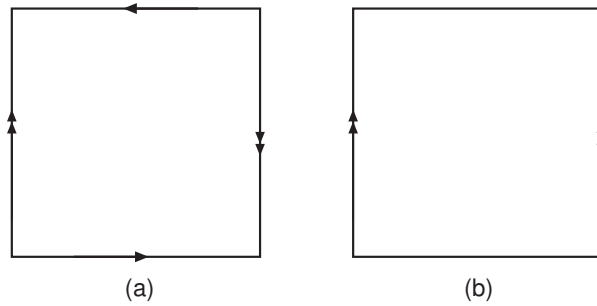


Figure 3: (a) A representation of the projective plane. Common arrows denote surfaces to be identified, together with the orientation. (b) The Möbius strip, shown for comparison.

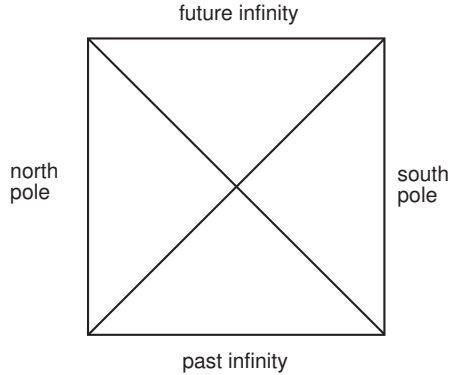


Figure 4: *Conformal diagram of de Sitter space.* The vertical axis represents conformal time, running from 0 to π . This version of the diagram is appropriate for a 4-dimensional spacetime, with θ and ϕ coordinates suppressed.

properties. The 3-sphere S^3 is the group manifold of the three dimensional spin group (and also $SU(2)$), and $\mathbb{R}P^3$ is correspondingly the group manifold of $SO(3)$. From our perspective, the standard framework of S^n spatial sections is the one of greatest interest, though this is largely an aesthetic judgement. There does not appear to be any obvious physical criteria for favouring one over the other.

There are a range of conformal representations one can adopt for de Sitter space [21]. Probably the simplest is the Carter–Penrose diagram, shown in figure 4. In this picture the temporal coordinate represents conformal time, and the spatial section represents the effective radial coordinate. A 2-sphere is suppressed at each point. If one wants to represent the simpler 2-dimensional de Sitter space, the diagram needs to be wrapped onto a cylinder. While this picture is instructive, we seek a picture that embodies some of the features of the Poincaré disk model. So, for example, geodesics should have a simple representation in terms of curves of constant (Minkowski) distance from some point. To achieve such a picture, we start by considering the spatial section at $T = 0$. This section is a ring of radius a , which is mapped onto a straight line in a $(1, 1)$ Lorentzian space via a stereographic projection. Null geodesics from this section are represented as 45° straight lines in Lorentzian space. Since geodesics from opposite points on the ring meet at infinity, we arrive at a boundary in the timelike direction defined by a hyperbola. This construction provides us with a Lorentzian view of de Sitter geometry. Timelike geodesics in de Sitter space are represented by hyperbolae that intersect the boundary at a (Lorentzian) right-angle (see figure 5).

There are many fascinating geometric structures associated with de Sitter geometry, many of which mirror those of non-Euclidean geometry. For example, one can always find a reflection that takes any point to the origin [22]. One can then prove a number of results at the origin, where the geodesics are all straight lines, and the results are guaranteed to hold at all points. A similar approach can be applied to anti-de Sitter space, except now the diagram is rotated through 90° , as it is the timelike direction that is formed from a stereographic unwrap-

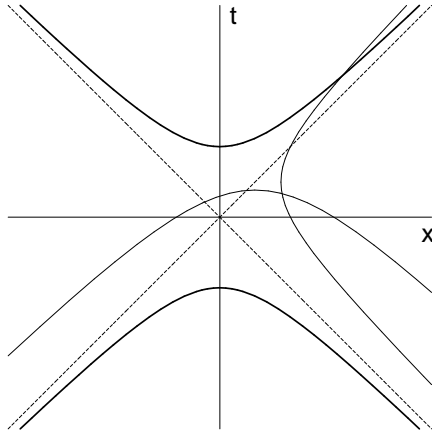


Figure 5: *The Lorentzian view of two-dimensional de Sitter space.* The boundary is defined by two hyperbolae (shown with thick lines). All geodesics through the origin are straight lines, and null geodesics are always straight lines at 45° . Two further geodesics, one spacelike and one timelike, are also shown. These are hyperbolae which do not pass through the origin. The timelike geodesic intersects the boundary in such a way that the two tangent vectors have vanishing Lorentzian inner product.

ping of a circle. A valuable mathematical tool for studying these geometries is provided by *conformal geometric algebra* [3, 23], which is essentially a Clifford algebra for the conformal space of two dimensions higher. So a 4-dimensional de Sitter spacetime is studied in the Clifford algebra of a 6-dimensional space with signature (2,4). Points, lines (including geodesics), planes and spheres are all represented by graded multivectors in the algebra, and union and intersection operations can be defined analogously to projective geometry [22].

The metric associated with the Lorentzian view of 2-dimensional de Sitter geometry has the conformally-flat structure

$$ds^2 = \frac{a^4}{(a^2 + x^2 - t^2)^2} (dt^2 - dx^2). \quad (4)$$

This makes it clear that null geodesics must remain as straight lines in the x - t plane. A similar line element is appropriate for four dimensional spacetimes, but these are not commonplace in the literature (except for the simple case of flat cosmologies). We finish this section by outlining the steps required to transform a standard FRW line element in the form

$$ds^2 = dt^2 - \frac{R(t)^2}{(1 + kr^2/4)^2} (dr^2 + r^2(d\theta^2 + \sin^2(\theta) d\phi^2)) \quad (5)$$

into the spacetime-conformal line element

$$ds^2 = \frac{1}{f^2} (dt^2 - dr^2 - r^2(d\theta^2 + \sin^2(\theta) d\phi^2)), \quad (6)$$

where f is a (dimensionless) function of t and r .

The first problem to address is that the r coordinate in equation (5) is assumed to be dimensionless. To rectify this we introduce a constant distance λ and replace the line element of (5) with

$$ds^2 = dt^2 - \frac{4\lambda^2 R(t)^2}{(\lambda^2 + kr^2)^2} (dr^2 + r^2(d\theta^2 + \sin^2(\theta) d\phi^2)). \quad (7)$$

Here t , r , λ and R all have units of distance (assuming $c = 1$). As usual, the constant k is either ± 1 or zero. Comparing the angular terms in equations (5) and (6) we see immediately that

$$\frac{r}{f} = \frac{2\lambda r R(t)}{\lambda^2 + kr^2}. \quad (8)$$

The coordinate transformation from (t, r) to (\mathbf{t}, \mathbf{r}) must satisfy

$$\begin{aligned} d\mathbf{t} &= f \cosh(u) dt + \frac{r}{r} \sinh(u) dr \\ d\mathbf{r} &= f \sinh(u) dt + \frac{r}{r} \cosh(u) dr. \end{aligned} \quad (9)$$

For flat cosmologies ($k = 0$) we simply set \mathbf{t}/λ equal to the conformal time η , where

$$\eta = \int_0^{\mathbf{t}} \frac{dt'}{R(t')}, \quad (10)$$

and we then have $r = r$ and the hyperbolic angle u is set to zero. For non-flat cosmologies it is perhaps surprising to find that u is non-zero. That is, there is a mismatch between the conformal coordinate frame and the cosmological frame. It follows that the conformal time η is not the same as the time-like conformal coordinate \mathbf{t} .

Using the integrability conditions for the coordinate transformations, and setting the initial singularity to $\mathbf{t} = 0$, the following solutions are found in the three cosmological scenarios [4]:

$$\begin{aligned} f &= \frac{\mathbf{t}}{R \sin(\eta)} = g \left(\frac{2\lambda \mathbf{t}}{\lambda^2 + r^2 - \mathbf{t}^2} \right) \frac{\mathbf{t}}{\lambda} && \text{closed} \\ f &= \frac{2\lambda}{R} && \text{flat} \\ f &= \frac{\mathbf{t}}{R \sinh(\eta)} = \bar{g} \left(\frac{2\lambda \mathbf{t}}{\lambda^2 + \mathbf{t}^2 - r^2} \right) \frac{\mathbf{t}}{\lambda} && \text{open.} \end{aligned} \quad (11)$$

Here g and \bar{g} are functions (in general elliptic) satisfying differential equations depending on the matter content.

3 A boundary condition for conformal time

All cosmological models are conformally flat, and can all be interchanged via conformal transformations. Furthermore, all models containing a cosmological constant, and which do not recollapse, will tend towards a de Sitter end state. Such models should fit neatly within the conformal diagram of figure 5 with future infinity represented by the upper hyperbolic boundary. A flat section

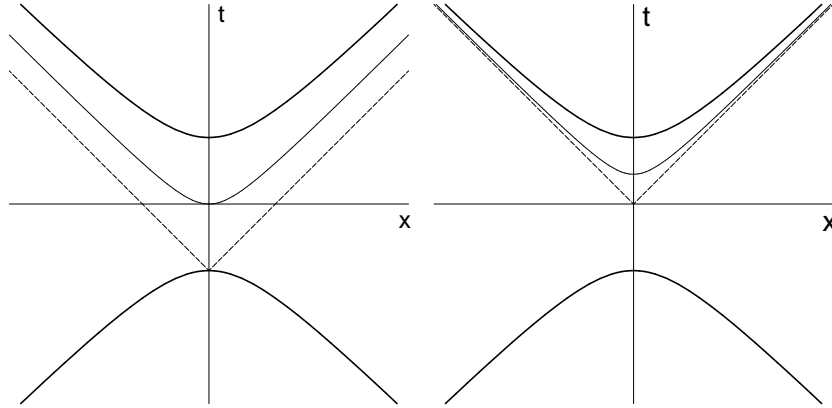


Figure 6: *Flat and open cosmological models.* de Sitter space contains sections representing both flat and open spacetimes. A flat spacetime (left) consists of the space contained inside a light-cone located on past infinity. An open spacetime fits inside the lightcone from the origin. Both pictures can be used to illustrate cosmological models, with the initial singularity represented by a hyperbolic spacelike surface. An example of these surfaces is shown on each diagram.

of de Sitter space corresponds to a region contained within a light cone from a point located on the boundary at past infinity (see figure 6). Surfaces of constant cosmic time are represented as hyperbolae, any one of which can then be chosen to represent the initial singularity. Similarly, an open section of de Sitter space is represented by the area inside a light-cone from a point in the middle of the de Sitter picture. An open Λ -cosmology will have the initial singularity located on a spacelike hyperbola.

The diagrams for flat and open cosmologies make it clear that one is not employing the full de Sitter geometry in a symmetric manner. Closed models, on the other hand, can be given a more natural embedding, since their initial singularity can be represented by a spacelike surface placed anywhere in the conformal diagram of figure 5. For all but one choice of position of the initial singularity, the future asymptotic de Sitter state of the model will not match onto the future infinity boundary of the conformal diagram. However, suppose that we insist that $t = 0$ represents the initial singularity. In this case the entire history of the universe can be conformally mapped into the top half of the de Sitter diagram. We suggest that this gives a natural boundary condition, as the centre of the diagram is the most natural, symmetric place to locate the big-bang singularity. (This choice also hints at a possible pre-big bang phase, but this is not explored here.) It might be thought that our proposal just amounts to a choice of coordinates. However, we now demonstrate that it has physically measurable consequences, and also that it can be recovered via an eigenvalue-type condition on the underlying equations, hinting at its origin as a possible quantisation condition.

One immediate physical consequence of our proposal is that any photon emitted from the initial singularity may travel a maximum of precisely one-

quarter of the way round the universe in the entire future evolution of the universe. An alternative way of saying this is that the past horizon projected back to $t = 0$ should cover half of the de Sitter geometry. If we let ϕ denote an equatorial angle on a 3-sphere, a photon travelling round the equator will satisfy

$$\frac{d\phi}{dt} = \frac{1}{R}, \quad (12)$$

where t is cosmic time. Traversing the entire universe corresponds to running from $0 \leq \phi \leq 2\pi$. If a photon is only to travel one-quarter of the way round we therefore require that

$$\int_0^\infty \frac{dt}{R} = \int_0^\infty \frac{dR}{R(-1 + \Lambda R^2/3 + 8\pi\rho R^2/3)^{1/2}} = \pi/2. \quad (13)$$

That is, the total available conformal time is $\pi/2$. This constraint can also be arrived at through an alternative route that works entirely within the conformal representation of cosmological models [22]. A de Sitter space centred on $t = 0 = \tau$ has the conformal line element

$$ds^2 = \frac{12\lambda^2}{\Lambda(\lambda^2 + r^2 - \tau^2)^2} (dt^2 - dx^2 - dy^2 - dz^2). \quad (14)$$

Clearly the only forms for f in equation (11) that have any chance of matching onto this final state are those for a closed universe. Furthermore, the function g must satisfy

$$\lim_{\chi \rightarrow \infty} g(\chi) = \left(\frac{\lambda^2 \Lambda}{3} \right)^{1/2} \frac{1}{\chi} \quad (15)$$

where

$$\chi = \frac{2\lambda t}{\lambda^2 + r^2 - \tau^2} = \tan(\eta). \quad (16)$$

But since

$$g = \frac{\lambda}{R \sin(\eta)} \quad (17)$$

we must then have $R \cos(\eta)$ tending to a constant at large times. This is only possible if η tends to $\pi/2$, recovering our earlier boundary condition. This derivation is instructive in that it reveals how the constraint can be imposed as a straightforward boundary condition on a differential equation. In this case, the equation for $g(\chi)$ is

$$\chi^2(1 + \chi^2) \left(\frac{dg}{d\chi} \right)^2 + \frac{d}{d\chi}(g^2 \chi) = \frac{8\pi G \lambda^2 \rho}{3} + \frac{\lambda^2 \Lambda}{3}. \quad (18)$$

The task then is to solve this equation subject to the boundary condition that g falls off as $1/\chi$ for large χ . Viewed this way the constraint can be thought of as a ‘quantisation condition’ applied as the universe is formed, which one might hope would emerge from a quantum theory of gravity.

In order to understand the implications of our boundary condition, we turn to considering flow lines in the $(\Omega_M, \Omega_\Lambda)$ plane (see figure 7). The plots show a series of flow lines starting from $\Omega_M = 1, \Omega_\Lambda = 0$, refocusing around the spatially flat case, $\Omega_M + \Omega_\Lambda = 1$. One can show that, for a large range

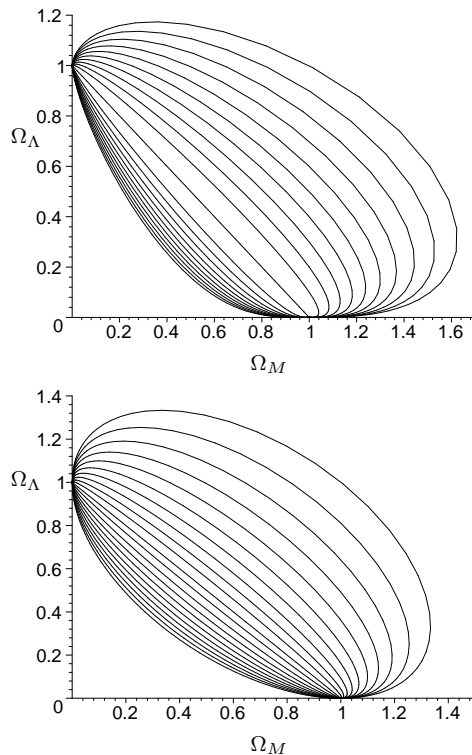


Figure 7: Evolution curves in the $(\Omega_M, \Omega_\Lambda)$ plane. The left-hand plot is for dust, and the right-hand plot is for radiation. In both cases the curves converge to $\Omega_\Lambda = 1$, representing a late-time de Sitter phase.

of initial conditions, by the time we reach the current value of $\Omega_M \approx 0.3$ most models are not far off spatial flatness. This prediction contrasts with models without a cosmological constant, where any slight deviation from the critical density in the early universe is scaled enormously by the time we reach the present epoch, implying that the parameters in the early universe are highly fine-tuned. The presence of a cosmological constant therefore goes some way to solving the flatness problem on its own, without the need to invoke inflation.

Each of the flow lines in figure 7 has a different value for the total evolved conformal time. Imposing a constraint on this picks out a single preferred trajectory, resulting in the two curves shown in figure 8 (one for matter-filled and one for radiation-filled). As the universe is expected to be matter dominated for most of its history, the solid line in figure 8 is the more physically relevant one. Taking the present-day energy density to be around $\Omega_M = 0.3$, we see that $\Omega_\Lambda =$ is predicted to be around $\Omega_\Lambda \approx 0.83$. That is, a universe that is closed at around the 10% ratio. Such a prediction is reasonably close to the observed value, though it is ruled out by the most recent experiments [1]. In order to improve the prediction, we need to use up a greater fraction of the conformal time before we enter the matter-dominated phase. Such a process is also necessary to solve the horizon problem, and the simplest means of achieving

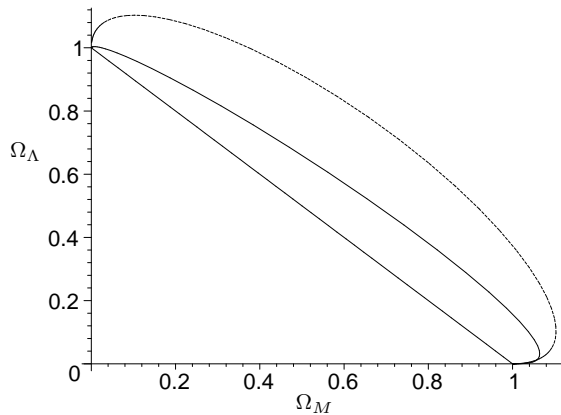


Figure 8: *Critical paths as predicted by the de Sitter embedding.* The solid line represents a matter-dominated universe, and the broken line shows radiation, for comparison. The straight line is the critical case of spatial flatness. By the time we reach $\Omega_M \approx 0.3$ the universe has been driven close to critical density.

this is via an inflationary phase.

4 Scalar field inflation

One can argue about the extent to which inflation really does solve the original problems it was intended to. For example, we have seen that the presence of a cosmological constant alone goes a long way to solving the flatness problem, without requiring inflation to put the universe in an effective de Sitter phase. But when it comes to generating structure on scales greater than the horizon, inflation is currently the only option. The simplest model of inflation models the matter content as a real, time-dependent, homogeneous massive scalar field. For a range of initial conditions this system shows the expected inflationary behaviour. The evolution equations for this model are

$$\dot{H} + H^2 - \frac{\Lambda}{3} + \frac{4\pi G}{3}(2\dot{\phi}^2 - m^2\phi^2) = 0 \quad (19)$$

and

$$\ddot{\phi} + 3H\dot{\phi} + m^2\phi = 0. \quad (20)$$

Given a solution to the pair of equations (19) and (20), a new solution set is generated by scaling with a constant σ and defining

$$H'(t) = \sigma H(\sigma t), \quad \phi'(t) = \phi(\sigma t), \quad m' = \sigma m, \quad \Lambda' = \sigma^2 \Lambda. \quad (21)$$

This scaling property is valuable for numerical work, as a range of situations can be covered by a single numerical integration. A range of physical quantities are invariant under changes in scale, including the conformal time η as can be seen from equation (10). The scaling property does not survive quantisation, however, so has to be employed carefully when considering vacuum fluctuations.

The initial conditions for equations (19) and (20) are usually set at the start of the inflationary period, where they are viewed as arising from some form of quantum gravity interaction. But in order to apply our boundary condition we need to track the equations right back to the initial singularity, as this is the only way that we can keep track of the total conformal time that has elapsed. Evolving the inflationary equation backwards in time is entirely justified, as we do not expect quantum gravity to play a role until much earlier in the history of the universe. Inflation on its own does not eliminate singularities from cosmology [12, 13]. Furthermore, by specifying initial conditions around the singularity, the states of the fields at the onset of inflation are fully determined by a pair of parameters, making the model highly predictive.

As the universe emerges from the big bang the dominant behaviour of H is to go as $1/(3t)$. Equation (19) then implies that ϕ must contain a term going as $\ln(t)$. But this in turn implies that H must also contain a term in $t \ln(t)$, in order to satisfy equation (20). Working in this manner we conclude that a series expansion in powers of t and $\ln(t)$ is required to describe the behaviour around the singularity. At this point it is convenient to define the dimensionless variables

$$u = \frac{t}{t_p}, \quad \mu = \frac{m}{m_p} \quad (22)$$

with t_p and m_p the Planck time and mass respectively. The series expansion about the singularity at $t = 0$ can now be written

$$H(u) = \frac{1}{t_p} \sum_{i=0}^{\infty} H_i(u) \ln^i(u), \quad \phi(u) = \frac{1}{l_p} \sum_{i=0}^{\infty} \phi_i(u) \ln^i(u), \quad (23)$$

which ensures that the expansion coefficients are all dimensionless. Substituting these into the two evolution equations, and setting each coefficient of $\ln(u)$ to zero, we establish that

$$H_1 = -u \frac{dH_0}{du} - uH_0^2 + \frac{u\Lambda}{3} - \frac{8\pi u}{3} \left(\frac{d\phi_0}{du} \right)^2 - \frac{16\pi\phi_1}{3} \frac{d\phi_0}{du} - \frac{8\pi\phi_1^2}{3u} + \frac{4\pi\mu^2 u\phi_0^2}{3}, \quad (24)$$

with further algebraic equations holding for H_2, ϕ_2, H_3, ϕ_3 , and so on. So, by specifying H_0, ϕ_0 and ϕ_1 , all the remaining terms in the solution are fixed. The aim now is to choose the three input functions to ensure that successive terms in the series get progressively smaller. This provides just the right number of equations to specify all coefficients, save for two arbitrary coefficients in ϕ_0 . This results in a series expansion controlled entirely by two arbitrary constants, which is the expected number of degrees of freedom once we have fixed the singularity to $t = 0$. In order to generate curvature it turns out that the input functions need to be power series in $u^{1/3}$, which ensures that the scale factor goes as $u^{1/3}$ at small times. The series solution is only required to find suitable initial conditions for numerical evolution, so only the first few terms are required.

Expanding up to order $u^{5/3}$ we find that

$$H_0 = \frac{1}{3u} + \frac{32\sqrt{3\pi}}{27}b_4u^{1/3} + \left(\frac{2\mu^2}{81} + \frac{\Lambda}{3} + \frac{4\pi}{3}\mu^2b_0^2 + \frac{4\sqrt{3\pi}}{27}\mu^2b_0 \right) u - \frac{6656\pi b_4^2}{891}u^{5/3}, \quad (25)$$

$$\phi_0 = b_0 + b_4u^{4/3} - \frac{118\sqrt{3\pi}b_4^2}{99}u^{8/3} - \frac{1}{1296\pi} \left(11\sqrt{3\pi}\mu^2 - 54\sqrt{3\pi}\Lambda - 216\sqrt{3}\pi^{3/2}\mu^2b_0^2 + 36\pi\mu^2b_0 \right) u^2 \quad (26)$$

and

$$\phi_1 = -\sqrt{\frac{1}{12\pi}} - \frac{\mu^2}{216\pi} \left(-\sqrt{3\pi} + 36\pi b_0 \right) u^2. \quad (27)$$

Under scaling the three key parameters in the model transform as $\mu \mapsto \sigma\mu$, $b_0 \mapsto b_0$, and $b_4 \mapsto \sigma^{4/3}b_4$. This scaling transformation for b_4 is entirely as expected, given that it is the coefficient of $u^{4/3}$ in the series for ϕ_0 . It follows that the quantity $b_4/\mu^{4/3}$ is scale invariant.

The fact that b_4 controls the curvature can be seen from equation (1) which, to leading order, yields

$$\frac{R}{l_p} = \frac{1}{\mu} \left(\frac{2187}{12544\pi} \right)^{1/4} \left(-\frac{\mu^{4/3}}{b_4} \right)^{1/2} (\mu u)^{1/3} + \dots \quad (28)$$

Clearly, the arbitrary constant b_4 must be negative for a closed universe. The terms on the right-hand side of equation (28) are all scale invariant, apart from the first factor of μ^{-1} . In figure 9 we illustrate Hubble function entry into the inflationary regime for typical values of b_0 and $b_4/\mu^{4/3}$ of interest. We see that the onset of inflation corresponds to $\mu u \approx 0.1$. In order to generate perturbations consistent with observation the scalar field must have a mass of the order of $10^{-6}m_p$. It follows that the onset of inflation occurs at a time of around 10^5 Planck times. The radius of the universe at the onset of inflation is then given approximately by

$$R \approx \frac{0.2}{\mu} l_p, \quad (29)$$

and so is of order 10^5 Planck lengths. Inflation therefore starts at an epoch well into the classical regime. Quantum gravity effects would be expected to be relevant when the radius of the universe is of the order of the Planck scale, which occurs when $u \approx \mu^2$ and is well before any inflationary period (for physical values of μ). We are therefore quite justified in running the evolution equations back past the inflationary regime, and right up to near the initial singularity. It is only when $R = l_p$ that the equations will break down, and we would look to quantum gravity to explain the formation of the initial, Planck-scale sized universe. Indeed, we would argue more strongly that we *have* to run the equations backwards in time to well before the start of inflation before reaching an epoch where new physics could be expected to enter the problem.

As the universe is described by a 3-sphere of radius R , the total volume of the universe is given to leading order by

$$V = 2\pi^2 \left(\frac{2187}{12544\pi} \right)^{3/4} \frac{l_p^3}{(-b_4)^{3/2}} u + \dots \quad (30)$$

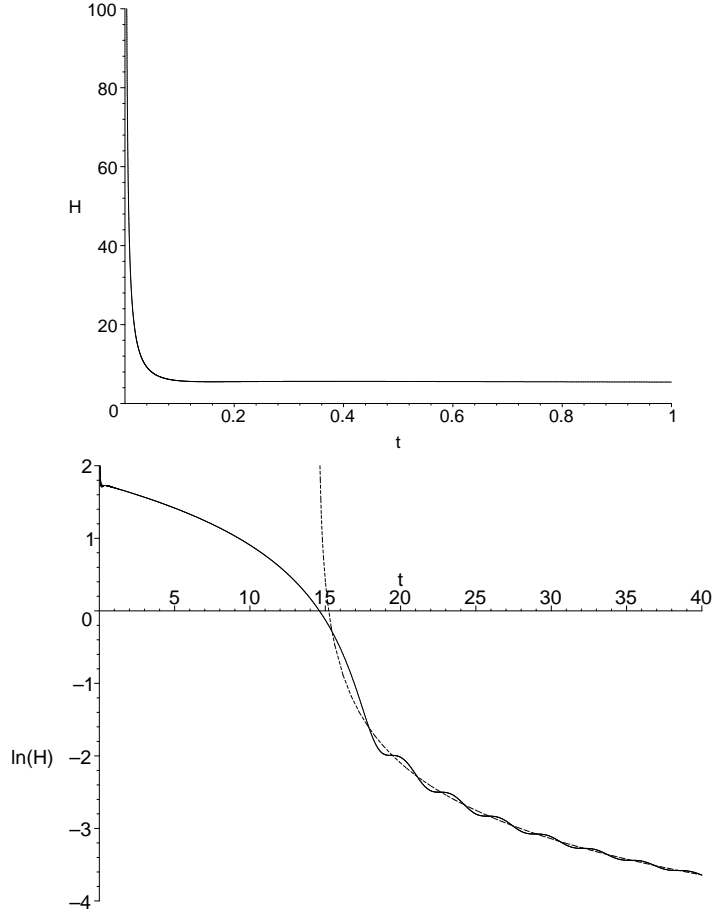


Figure 9: *Hubble function entry into and exit from the inflationary regime.* The Hubble function emerges from the big bang going as $1/3t$. As H falls it quickly enters the inflationary region, during which it falls linearly. As the inflationary era ends the density and pressure start oscillating around values for a matter-dominated cosmology. The effective singularity for this dust cosmology is displaced from $t = 0$. The broken line plots the natural log of $2/3(t - 14.56)$. Time t is measured in units of t_p , and H in units of t_p^{-1} . The input parameters were set to $b_0 = 2.48$, $b_4 = -0.51$ and $m = m_p$ ($\mu = 1$).

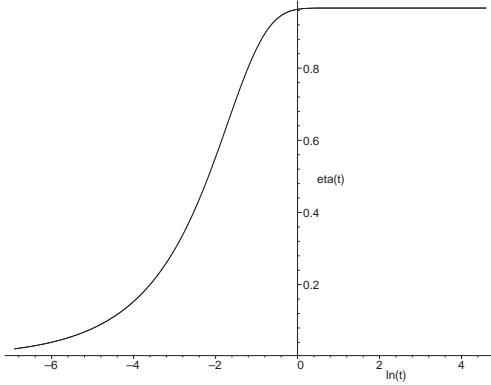


Figure 10: *Evolution of the conformal time $\eta(t)$ as a function of $\ln(t)$.* The parameters for the model are as given in figure 9 and again t is measured in units of the Planck time. This plot sets $\mu = 1$, so the time variable must be scaled to correspond to more physical values of $\mu \approx 10^{-6}$.

Following from this, an interesting calculation we can perform in a closed universe is to find the total energy contained within it in the scalar field. By integrating the energy density we find that

$$E_{\text{tot}} = \frac{\pi}{12} \left(\frac{2187}{12544\pi} \right)^{3/4} \frac{1}{(-b_4)^{3/2}} \frac{\hbar}{t} + \dots \approx 0.03 \left(\frac{-\mu^{4/3}}{b_4} \right)^{3/2} \frac{\hbar}{\mu^2 t}, \quad (31)$$

and when the scale-invariant quantity $b_4/\mu^{4/3}$ is of order unity (as required for physical models) we have

$$E_{\text{tot}} \approx \frac{0.03 \hbar}{\mu^2 t}. \quad (32)$$

This tells us that the action Et is very large, when measured in units of \hbar . This is reassuring, as it means we are justified in treating the universe on the whole as a classical object.

The plots in figure 9 illustrate the general behaviour of the Hubble function H . As the universe emerges from the big bang the energy density in the scalar field is dominated by the $\dot{\phi}$ term, and the field behaves as if it is massless. It follows that H initially falls as $1/(3t)$. But once H has fallen sufficiently far we enter a region in which $m^2\phi^2$ starts to dominate over $\dot{\phi}^2$. These are suitable initial conditions for the universe to enter an inflationary phase. By varying b_0 , b_4 and μ we control both the values of the fields as we enter the inflationary period, and how long the inflationary period lasts. The cosmological constant plays no significant role in this part of the evolution. The dynamics displayed in this figure is quite robust over a range of input parameters. A significant point here is that we enter the inflationary regime from a region of high H , as opposed to the $H \approx 0$ value favoured in some models of quantum cosmology. We therefore never enter the regions of parameter space where the chaotic evolution noticed by Page [24] and Cornish & Shellard [25] is relevant.

The typical behaviour as we exit the inflationary region is also shown in figure 9. The end of inflation is characterised by $H \approx \mu$. Beyond this point the scalar field enters an oscillatory phase, with the time-averaged fields satisfying

the conditions for a simple matter-dominated cosmology. In this case H can be approximated by a curve going as $2/3(t - t_0)$, describing a dust model with a displaced origin. The universe then appears as if it has been generated by an ‘effective’ big bang at a later time. Around this time we expect reheating effects to start to dominate, so that in reality the universe must pass over to a radiation-dominated era. But the naive ‘effective big bang’ concept is useful for extracting some qualitative predictions from our model [4]. Figure 10 shows the evolution of conformal time for the model depicted in figures 9. As the universe emerges from the initial singularity, η grows at $t^{2/3}$. But once the inflationary region is entered, $R(t)$ starts to increase rapidly. So the conformal time, which involves the time integral of R^{-1} , quickly saturates. So if η has not reached $\pi/2$ before R has inflated significantly, the universe will have to exist for an extremely long time to reach the boundary value of $\pi/2$. Similarly, in this simple picture, we can obtain the prediction for Λ given in equation (2) (for details see [4]). We note with the number of e-folds $N \approx 46$, then $\Lambda \sim 10^{-122} l_{\text{pl}}^{-2}$, which is in exactly the right ball park!

5 The power spectrum

In [4] we give an account of how to extract the power spectrum of primordial fluctuations, using the various approximations that have become standard in the literature. As an example of the type of results achieved, we show in figure 11 a comparison of our computed scalar power spectrum with the WMAP best fit power law and running spectral index fits. The vertical normalisations for these fits have been chosen arbitrarily, since it is the shape of the spectrum at large k which is of greatest interest here. The running spectral index graph is interesting in that it suggests that this model is attempting to emulate both the cutoff at low k , as well as the reduced power at large k , which occurs in our model. The latter occurs as a result of computing the perturbation spectrum more accurately than usual in this regime, and is not a specific feature of using a closed universe model.

In figure 12 we show a predicted CMB power spectrum from our model, in comparison with the WMAP results and the prediction from a strictly power law initial spectrum. This model has $\Omega_0 = 1.04$, so is consistent with WMAP at the 1σ level. We also take $\Omega_b h^2 = 0.0224$, $h = 0.60$ and $\Omega_{\text{cdm}} h^2 = 0.110$. Together these yield a value of $\Omega_{\text{cdm}} = 0.306$, which is reasonable, although of course the H_0 value is rather low. It can be seen that our predicted CMB spectrum is in much better agreement with the WMAP results at low ℓ than the predictions from the primordial power law. This could be taken as good evidence for our model, except that it is necessary to check the correctness of the approximations we have used in calculating the perturbation power spectrum. This work is currently in progress, but we end this paper with a brief discussion of some of the technical problems involved.

The starting point for calculating the scalar curvature spectrum in a simple flat model is to write the linearised perturbed action in the form [26]

$$\delta_2 S = \frac{1}{2} \int d\eta d^3 x \left(v'^2 - \eta^{ij} v_{,i} v_{,j} + \frac{z''}{z} v^2 \right). \quad (33)$$

Here v is a gauge-invariant combination of matter and metric perturbations,

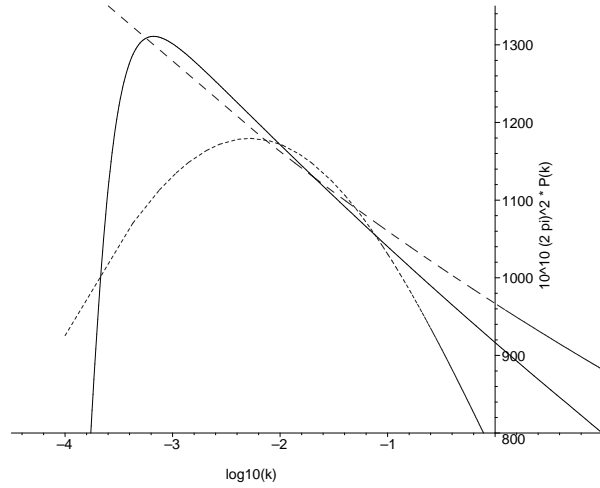


Figure 11: *Comparison of the scalar power spectrum of curvature perturbations, $\mathcal{P}_{\mathcal{R}}(k)$, with power law models.* The function plotted is $10^{10}(2\pi)^2\mathcal{P}_{\mathcal{R}}(k)$ as a function of $\log_{10}(k)$, assuming $h = 0.65$. The solid line represents the numerical predictions from our model. The long dashes represent the best fit power law ($n_s = 0.96$) and the short dashes are the WMAP running spectral index best fit. Notice that the vertical scale runs from 800 to 1300, so the differences are slightly exaggerated.

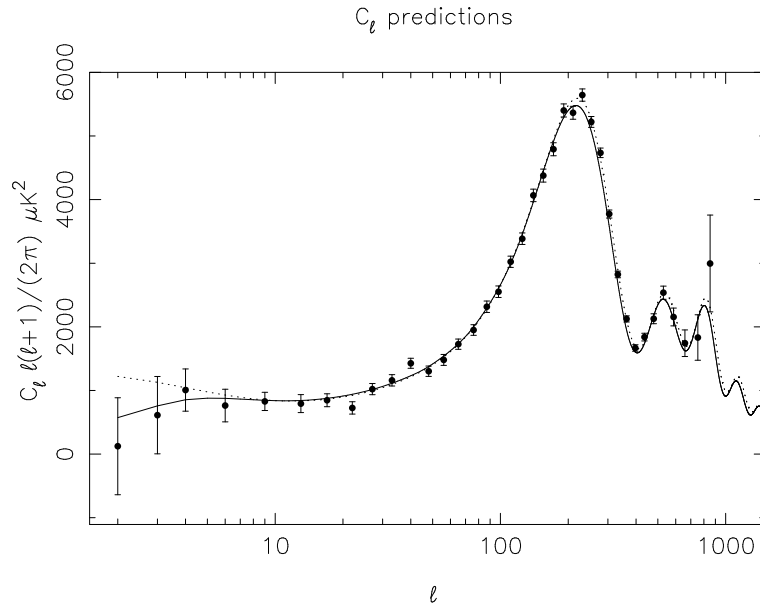


Figure 12: *CMB power spectrum for a model with $\Omega_0 = 1.04$* The parameters are discussed in the text. The experimental points shown with 1σ error bars are the WMAP results [1] and the dashed curve corresponds to the best fit Λ CDM power law CMB power spectrum as distributed in the WMAP data products.

dashes denote the derivative with respect to conformal time, and z is defined by $z = \phi'_0/H$, where ϕ_0 is the unperturbed field. By working with this action the entire problem is reduced to one of analysing a scalar field with a time-dependent mass term. This approach generalises to the non-flat case, although here the definition of z becomes more complicated [27]. Also, for closed models, the mode expansions necessary to carry out quantisation have to be performed using spatial sections given by the 3-sphere S^3 , so that the ‘comoving wavenumber’ k takes on integer values, with $k = 3$ its lowest (non-gauge) value. The mode equations found this way are very complicated, but retain the general form

$$v_k'' + (k^2 - f(\eta, k)) v_k = 0, \quad (34)$$

where in the flat case $f(\eta, k)$ would be z''/z , and in all cases $f(\eta, k)$ is calculable from knowledge of the background evolution.

The challenge now is to find suitable ‘quantum initial conditions’ so that after evolution through inflation, the variables v_k can be used to find the perturbation spectrum. To achieve this involves a mode decomposition of v_k into positive and negative frequencies. The standard way to approach this is to assume that in the asymptotic past the background is either Minkowski or de Sitter, so that one knows the correct vacuum to choose. But this is clearly inappropriate here, as looking back in time we encounter the initial singularity.

The question of how to proceed in the absence of any asymptotic notion of the vacuum state has been widely discussed. One simple approach is provided by Hamiltonian diagonalisation, where on each time slice modes are decomposed into positive and negative energy states by the Hamiltonian operator. But this technique tends to overestimate the particle production rate. A clear way to proceed was developed by Parker and Fulling [28, 29] and introduces the concept of an adiabatic vacuum. The application of this to the present case is complicated, but feasible, and initial results support a low- k cutoff, though with less pronounced effects than we have found using the standard approximate techniques. This will be the subject of a future publication.

References

- [1] D.N. Spergel et al. First year Wilkinson anisotropy probe (WMAP) observations: Determination of cosmological parameters. *Astrophys. J. Suppl.*, 148:175, 2003.
- [2] A.N. Lasenby, C.J.L. Doran, and S.F. Gull. Gravity, gauge theories and geometric algebra. *Phil. Trans. R. Soc. Lond. A*, 356:487–582, 1998.
- [3] C.J.L Doran and A.N. Lasenby. *Geometric Algebra for Physicists*. Cambridge University Press, 2003.
- [4] A.N. Lasenby and C.J.L. Doran. Closed universes, de Sitter space and inflation. astro-ph/0307311, 2003.
- [5] D.A. Brannan, M.F. Espleen, and J.J. Gray. *Geometry*. Cambridge University Press, 1999.
- [6] C.J. Isham and J.E. Nelson. Quantization of a coupled Fermi field and Robertson-Walker metric. *Phys. Rev. D*, 10(10):3226, 1974.

- [7] G. Efstathiou. Is the low CMB quadrupole a signature of spatial curvature? *MNRAS*, 343:L95, 2003.
- [8] A.A. Starobinsky. Spectrum of initial perturbations in open and closed universes. In M. Khlopov, M.E. Prokhorov, A.A. Starobinsky, and J. Tran Thanh Van, editors, *Cosmoparticle Physics*, page 43. Edition Frontiers, 1996.
- [9] G. Efstathiou. A maximum likelihood analysis of the low CMB multipoles from WMAP. *MNRAS*, 348:885, 2004.
- [10] C.R. Contaldi, M. Peloso, L. Kofman, and A. Linde. Suppressing the lower multipoles in the CMB anisotropies. *JCAP*, 07(002):1, 2003.
- [11] J. Uzan, A. Riazuelo, R. Lehoucq, and J. Weeks. Cosmic microwave background constraints on lens spaces. *Phys. Rev. D.*, 69(4):043003, February 2004.
- [12] R.H. Brandenberger. Principles, progress and problems in inflationary cosmology. *AAPPS Bull.*, 11:20, 2001.
- [13] A. Border, A.H. Guth, and A. Vilenkin. Inflationary spacetimes are not past-complete. *Phys. Rev. Lett.*, 90:151301, 2003.
- [14] R. Penrose. *The Road to Reality*. Jonathan Cape, 2004.
- [15] A. Linde. Can we have inflation with $\Omega > 1$? *J. Cosmol. Astropart. Phys.*, 5:2, 2003.
- [16] J. Uzan, U. Kirchner, and G.F.R. Ellis. WMAP data and the curvature of space. *MNRAS*, 344:L65, 2003.
- [17] G.F.R. Ellis, W. Stoeger, P. McEwan, and P. Dunsby. Dynamics of inflationary universes with positive spatial curvature. *Gen. Rel. Grav.*, 34:1445, 2002.
- [18] G.F.R. Ellis, P. McEwan, W. Stoeger, and P. Dunsby. Causality of inflationary universes with positive spatial curvature. *Gen. Rel. Grav.*, 34:1461, 2002.
- [19] D. Klemm and L. Vanzo. Aspects of quantum gravity in de Sitter spaces. hep-th/0407255, 2004.
- [20] B. McInnes. De Sitter and Schwarzschild-de Sitter according to Schwarzschild and de Sitter. *JHEP*, 0309:009, 2003.
- [21] N.D. Birrell and P. C. W. Davies. *Quantum Fields in Curved Space*. Cambridge University Press, 1982.
- [22] A.N. Lasenby. Conformal geometry and the universe. *Phil. Trans. R. Soc. Lond. A*, to appear, 2003.
- [23] C. Doran, A. Lasenby, and J. Lasenby. Conformal geometry, Euclidean space and geometric algebra. In J. Winkler and M. Niranjana, editors, *Uncertainty in Geometric Computations*, pages 41–58. Kluwer Academic Publishers, Boston, 2002.

- [24] D.N. Page. A fractal set of perpetually bouncing universes. *Class. Quant. Grav.*, 1:417, 1984.
- [25] N. Cornish and E.P.S. Shellard. Chaos in quantum cosmology. *Phys. Rev. Lett.*, 81:2371, 1998.
- [26] V. F. Mukhanov, H. A. Feldman, and R. H. Brandenberger. Theory of cosmological perturbations. *Phys. Rep.*, 215:203–333, 1992.
- [27] D. Zhang and C. Sun. The exact evolution equation of the curvature perturbation for closed universe. astro-ph/0310127, 2003.
- [28] L. Parker. Quantized fields and particle creation in expanding universes. i. *Phys. Rev.*, 183:1057–1068, 1969.
- [29] S.A. Fulling. *Aspects of Quantum Field Theory in Curved Space-Time*. Cambridge University Press, 1989.